Comparison of frequency domain methods for discrete-time, linear time-varying system with invariant eigenvalues

PRZEMYSLAW ORLOWSKI
Institute of Control Engineering
Szczecin University of Technology
Sikorskiego 37, 70-313 Szczecin
POLAND
orzel@ps.pl http://www.orzel.ps.pl

Abstract: **The main aim of this paper is to compare and evaluate frequency methods applicable for discrete-time (DT) linear time-varying (LTV) systems, in particular: two-dimensional (time, frequency) transfer function (2D-TF), time-averaged 2D-TF and approximated Bode diagrams calculated using SVD-DFT approach and power spectral density (PSD) properties. The main evaluation criteria is possible applicability to feedback system stability analysis. The paper begins from short theoretical background of frequency methods applicable for LTV systems. Further properties of these methods are compared and discussed on the basis of particular case of parameter controlled switching DT LTV system.**

Key-Words: **- discrete-time systems, time-varying systems, non-stationary systems, stability analysis, finite time horizon, frequency analysis**

1. INTRODUCTION

Properties of linear time-invariant (LTI) systems are unequivocally connected with eigenvalues of the system matrix, however for the linear time-varying (LTV) systems analysis have to be much more complex. Although many papers were recently published for slowly varying LTV systems, there was less attention for fast switching LTV systems. The notion of hazard is well known in the theory of logical circuits as instability or abnormality of the system connected to transition state and variable response time. Similar effects may occur also for dynamical systems (continuous and discrete) when the changes of parameters are sufficiently large and often.

Frequency methods are one of the most important tools for LTI systems analysis. Well-developed concepts and analytic methods for such systems cannot be in simple manner applied to LTV systems. Nevertheless until now there are only a few papers in these area [1], [2] published recently. LTV frequency system analysis focuses on following directions: two dimensional transfer function (2D-TF) introduced by Zadeh [3] and extended by followers, averaged transfer function (ATF) which can be obtained by time-averaging of 2D-TF [4], pseudo modal parameters analysis (PMP), which extends the concept of modal parameters for LTI systems to the time-varying case [5]. Constant eigenvalues are substituted by their time-varying equivalents. Third approach proposed [6] and analysed [7], [8], [4] by the author, called SVD-DFT approximated Bode diagrams, is generalization of frequency domain description for LTV system, compatible to classical Bode diagrams for LTI systems, which preserve feedback stability properties for LTV systems [7], [8].

Main aim of this paper is to compare 3 known methods for time-frequency domain analysis for linear time-varying, discrete-time systems. Particularly we try to show main strengths and weaknesses, with special emphasis placed on the 2D transfer function and SVD-DFT approach. Most of the properties are analysed on the basis on feedback stability for given discrete-time switching system with invariant eigenvalues. Superiority of the proposed SVD-DFT approach in respect to alternative existing methods, e.g. 2D-transfer function (3D Bode diagrams) and ATF are shown on numerical examples in section 4.

2. MODEL DESCRIPTION

Dynamic, discrete-time system can be given by set of difference equations, called the state space model

$$\mathbf{x}_p(k+1) = \mathbf{A}(k)\mathbf{x}_p(k) + \mathbf{B}(k)\mathbf{v}_p(k), \quad (1)$$

$$\mathbf{y}_p(k) = \mathbf{C}(k)\mathbf{x}_p(k) + \mathbf{D}(k)\mathbf{v}_p(k), \quad (2)$$

where $\mathbf{x}_p(k) \in \mathbb{R}^n$ is the state, $\mathbf{v}_p(k) \in \mathbb{R}^m$ is control, $\mathbf{y}_p(k) \in \mathbb{R}^p$ is output, initial conditions are equal to zero $\mathbf{x}_p(0)=\mathbf{0}$, $\mathbf{A}(k) \in \mathbb{R}^{n\times n}$, $\mathbf{B}(k) \in \mathbb{R}^{n\times m}$, $\mathbf{C}(k) \in \mathbb{R}^{p\times n}$, $\mathbf{D}(k) \in \mathbb{R}^{p\times m}$ are system matrices and the time horizon is finite $k = 1,2,...,N$.

The system (1-2) can be given alternatively e.g. using following matrix operator's notation:

$$\hat{\mathbf{y}} = \hat{\mathbf{T}}\hat{\mathbf{v}} = \left(\hat{\mathbf{C}}\hat{\mathbf{L}}\hat{\mathbf{B}} + \hat{\mathbf{D}}\right)\hat{\mathbf{v}} \quad (3)$$

where signals operators input $\hat{\mathbf{v}}$, state $\hat{\mathbf{x}}$ and output $\hat{\mathbf{y}}$ are written using column block vector form, e.g. signal $\hat{\mathbf{x}}$ can be written in following way:

$$\hat{\mathbf{x}} = \left[\mathbf{x}_p(0), \mathbf{x}_p(1), ..., \mathbf{x}_p(N-1)\right]^{\mathrm{T}} \quad (4)$$

System operators have following form

$$\hat{\mathbf{B}}=\begin{bmatrix}\mathbf{B}(0) & \mathbf{0} & \mathbf{0}\\ \mathbf{0} & \ddots & \mathbf{0}\\ \mathbf{0} & \mathbf{0} & \mathbf{B}(N-1)\end{bmatrix}\quad \hat{\mathbf{C}}=\begin{bmatrix}\mathbf{C}(0) & \mathbf{0} & \mathbf{0}\\ \mathbf{0} & \ddots & \mathbf{0}\\ \mathbf{0} & \mathbf{0} & \mathbf{C}(N-1)\end{bmatrix} \quad (5)$$

$$\hat{\mathbf{L}}=\begin{bmatrix}\mathbf{0} & \mathbf{0} & \cdots & \mathbf{0} & \mathbf{0}\\ \mathbf{I} & \mathbf{0} & \cdots & \mathbf{0} & \mathbf{0}\\ \mathbf{A}(1) & \mathbf{I} & \mathbf{0} & \vdots & \vdots\\ \vdots & \ddots & \mathbf{I} & \mathbf{0} & \mathbf{0}\\ \mathbf{A}(N-2)\cdot\ldots\cdot\mathbf{A}(1) & \cdots & \mathbf{A}(N-2) & \mathbf{I} & \mathbf{0}\end{bmatrix} \quad (6)$$

Operator $\hat{\mathbf{D}}$ can be written using block diagonal form similar to operators $\hat{\mathbf{B}}$ and $\hat{\mathbf{C}}$. The input-output operator $\hat{\mathbf{T}}$ is bounded operator from l_2 into l_2 and can be alternatively written in terms of set of impulse responses of a time-varying system taken at different times. For SISO system it takes the following form:

$$\hat{\mathbf{T}}=\begin{bmatrix}h(0,0) & 0 & \cdots & 0\\ h(1,0) & h(1,1) & \cdots & 0\\ \vdots & \vdots & \ddots & \vdots\\ h(N-1,0) & h(N-1,1) & \cdots & h(N-1,N-1)\end{bmatrix} \quad (7)$$

where $h(k_1,k_0)$ is system response to Kronecker delta $\delta(k-k_0)$ at time k_1.

3. LTV SYSTEMS TRANSFORMATIONS

2D Transfer Function (2D-TF)

One of the first attempts for analysis LTV systems in the frequency domain has been made by Zadeh [3] and developed by followers e.g. [9]. The time-varying transfer function has been defined by extending the Laplace transform to the varying impulsive response. The most general realization for continuous time systems is following generalized Weyl-symbol.

$$L^{(\alpha)}(t,f)=\int h\left(t+\left(\tfrac{1}{2}-\alpha\right)\tau,t-\left(\tfrac{1}{2}+\alpha\right)\tau\right)e^{-j2\pi f\tau}d\tau \quad (8)$$

where $\alpha\in\mathbb{R}$ is arbitrary real number, usually $|\alpha|\le 0.5$ and $h(t_1,t_0)$ is impulse response of the system taken at time t_1 for Dirac impulse shifted by t_0. In general above transformation does not satisfy some properties which hold for time invariant systems. For example multiplication in the frequency domain does not correspond to the convolution in the time domain. Equation (8) cannot be applied directly to discrete time systems, following equation can be used instead:

$$K^{(\alpha)}(\tau_l,f_k)=\sum_{n=1}^{N}\eta\left(\left(l+\left(\tfrac{1}{2}-\alpha\right)n\right)T_p,\left(l-\left(\tfrac{1}{2}+\alpha\right)n\right)T_p\right)e^{-j2\pi(k-1)(n-1)/N} \quad (9)$$

where $\tau_l=lT_p, f_k=\dfrac{(k-1)}{NT_p}, l=1,2,\ldots,N, k=1,2,\ldots,\dfrac{N}{2}$

Assuming that α=-0.5 (frequency dependent modulation), the time-frequency transfer function can be written in following form:

$$K^{(-0.5)}(\tau_l,f_k)=\sum_{n=1}^{N}h(n+\tau_l,\tau_l)e^{-j2\pi(k-1)(n-1)/N} \quad (10)$$

where $h(k_1,k_0)$ is response to Kronecker delta $\delta(k-k_0)$ at time k_1.

For systems defined on finite time horizon $k\in\{0,...,N-1\}$, the 2D-TF can be calculated from system input output operator in upper triangle form. The form is similar to the operator $\hat{\mathbf{T}}$ with the difference that $\hat{\mathbf{T}}$ has lower triangular form.

$$K^{(-0.5)}(\tau_l,f_k)=\{\kappa_{k,l}\in\mathbf{K}=\mathrm{DFT}\left[\breve{\mathbf{T}}\right],\quad \breve{\mathbf{T}}=\begin{bmatrix}h(0,0) & h(1,1) & \cdots & h(N-1,N-1)\\ h(1,0) & h(2,1) & \cdots & 0\\ \vdots & \vdots & \iddots & \vdots\\ h(N-1,0) & 0 & \cdots & 0\end{bmatrix}\} \quad (11)$$

where $\{\kappa_{k,l}\}$ is element from k^{th} row and l^{th} column of matrix $\mathbf{K}$.

Averaged Transfer Function (ATF)

It is difficult to analyse properties of the LTV system using 2D-TF. One dimensional approximation of 2D-TF can be obtained by averaging complex transform $K^{(\alpha)}(\tau_l,f_k)$ in respect to time [4]. Numerically it can be written as following mean:

$$G_A^{(\alpha)}(j\omega_k)=\frac{1}{N}\sum_{l=1}^{N}K^{(\alpha)}(\tau_l,f_k) \quad (12)$$

where l and m are arbitrary integers in a given range $l,m\in\{1,2,\ldots,N\}$. If α is unspecified it is assumed that α=-0.5 and $G_A(j\omega_k)=G_A^{(-0.5)}(j\omega_k)$, $\omega_k=2\pi f_k$. The definition of ATF for LTV system relies upon the assumption that every sample has the same importance and thus can be averaged with equal weights. The ATF can be divided into the magnitude and the phase plot, where the magnitude $|G_A^{(\alpha)}(j\omega_k)|$ can be interpreted as the selective amplification of the first harmonic in the output spectra for a given sinusoidal input. All the other components which exist only for time-varying systems are neglected.

SVD-DFT Transformation

The method is based on Singular Value Decomposition of the system operator. This spectral decomposition is a generalization for SVD of a matrix. For discrete-time systems and finite time horizon the operator is finite dimensional.

The relation between input and output power spectral density and the amplitude diagram is described by:

$$\mathbf{S}_{\mathbf{y}}(\omega_k) = \left|\mathbf{G}(\omega_k)\right|^2 \mathbf{S}_{\mathbf{v}}(\omega_k) \tag{13}$$

where following property can be proved [6], [7], [8]:

$$\mathbf{S}_{\mathbf{v}}(\omega_k) = \sum_{j=1}^{N} S_j(\omega_k) = \frac{1}{N}\sum_{j=1}^{N}\left|\mathrm{DFT}_k[\mathbf{v}_j]\right|^2 = \mathbf{1} \tag{14}$$

for $\omega_k = k/\left(2\cdot T_p \cdot N\right)$ and sampling period T_p, then

$$\left|\mathbf{G}(\omega_k)\right| = \sqrt{\mathbf{S}_{\mathbf{y}}(\omega_k)} \tag{15}$$

and after substituting

$$\mathbf{S}_{\mathbf{y}}(\omega_k) = \frac{1}{N}\sum_{j=1}^{N}\left|\mathrm{DFT}_{\mathrm{k}}[\mathbf{u}_j\sigma_j]\right|^2 \tag{16}$$

where σ_i is i^{th} singular value of $\mathbf{USV}^{\mathrm{T}} = \hat{\mathbf{T}}$ SVD decomposition.

Finally magnitude diagram can be computed from

$$\left|\mathbf{G}\left(\omega_k\right)\right| = \sqrt{\frac{1}{N}\sum_{j=1}^{N}\sigma_j^2\left|\mathrm{DFT}_{\mathrm{k}}[\mathbf{u}_j]\right|^2} \tag{17}$$

and phase diagram, can be approximated by

$$\varphi\left(\omega_k\right) = \arg\left(\sum_{j=1}^{N}\sigma_j\frac{\mathrm{DFT}_{\mathrm{k}}[\mathbf{u}_j]}{\mathrm{DFT}_{\mathrm{k}}[\mathbf{v}_j]}\right) \tag{18}$$

Information included in SVD-DFT diagrams cannot be extracted for specific time samples. ATF and SVD-DFT methods applied to LTI systems give diagrams almost identically as like the classical Bode diagrams, (under sufficiently large time horizon). Further we show that SVD-DFT method is more efficient tool for stability evaluation for feedback LTV system than ATF and 2D-TF methods.

4. ANALYSIS OF CONSTANT EIGENVALUES LTV SYSTEM

The system under consideration is discrete-time LTV system with constant eigenvalues located inside the unity circle on the complex plane.

In spite of the fact that eigenvalues of the system matrix $\mathbf{A}(k)$ are inside the unity circle on the complex plane, the stability of the system depends on the switching of the system. The parameter that determines the switching interval is κ. The following relations unequivocally define the model (1-2)

$$\mathbf{A}(k) = \mathbf{A}_{\kappa}, \mathbf{B}(k) = \begin{bmatrix}1 & 0\end{bmatrix}^{\mathrm{T}}, \mathbf{C}(k) = \begin{bmatrix}0 & 1\end{bmatrix}, \mathbf{D}(k) = 0 \tag{19}$$

where

$$\mathbf{A}_0 = \begin{bmatrix}2 & 1.2\\ -2 & -1\end{bmatrix}, \mathbf{A}_1 = \begin{bmatrix}-1 & -2\\ 1.2 & 2\end{bmatrix}, \mathbf{A}_2 = \begin{bmatrix}-1 & 1.2\\ -2 & -2\end{bmatrix},$$
$$\mathbf{A}_3 = \begin{bmatrix}2 & -2\\ 1.2 & -1\end{bmatrix},\ \kappa = \mathrm{floor}\left(\mathrm{rem}\left(\frac{k}{\varepsilon}, 4\right)\right) \tag{20}$$

Variable κ denotes round towards minus infinity of the remainder of k/ε after division by 4. The sampling period is equal to T_p=0.04. The eigenvalues of matrix $\mathbf{A}(k)$ are independent of parameter ε and equal $\lambda_1(k) = \lambda_2^*(k) = 0.5 + 0.3873\mathrm{i}$ for all k. Complex eigenvalues $\lambda_i(k) = \exp\left[-\delta_i\left(k\right)T_p + j\omega_i\left(k\right)T_p\right]$ of the system correspond to damping factor $\delta_i\left(k\right) \cong 11.5$ and natural frequency $\omega_i\left(k\right) \cong \pm 16.5$. The invariance of the values in respect to k wrongly suggests that properties of the system do not depend on ε and also the system has only one resonant frequency about 16.5 rad/s=2.6 Hz. Examples considered here show that it might be approximately true only for slowly time-varying systems but it is not true in general.

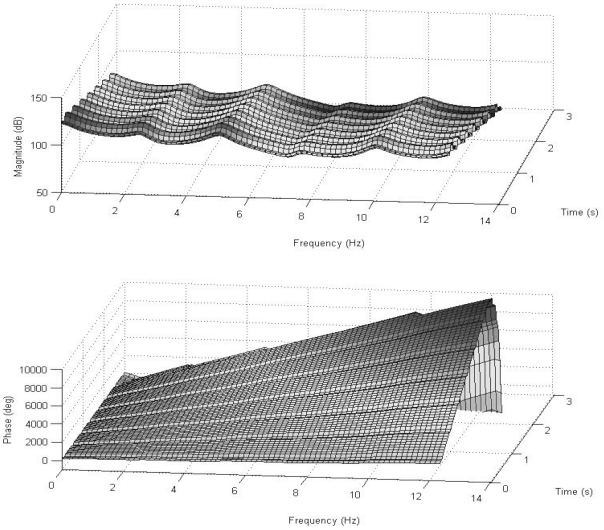

Fig. 4.1. 3D Bode diagrams determined for constant eigenvalues system (19-20) with parameters ε=2.5 and N=150.

To see how the parameter ε effects the stability of the system, the analysis will be carried out for 4 following values of parameter ε= 2.5, 2.93, 3 and 20.

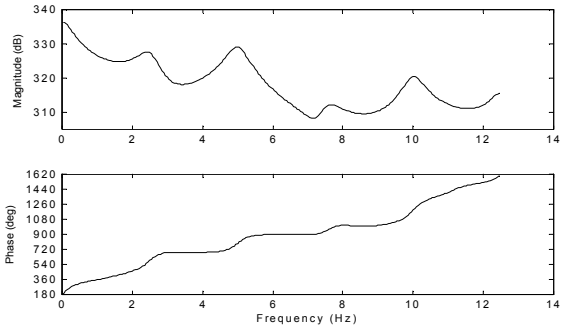

Fig. 4.2. Bode diagrams determined for discrete constant eigenvalues system (19-20) with parameters ε=2.5 and N=500.

When the parameter ε takes the value ε=2.5 the system becomes unstable. The 2D-TF defined by eq. (10) divided into magnitude and phase plot is depicted on Fig. 4.1. Fig. 4.2 shows approximated Bode diagrams obtained using SVD-DFT method. High amplification levels on amplitude diagrams on Fig. 4.2 acknowledge negative stability of the system. When the system is

unstable the magnification level in the amplitude diagram strongly depends on the length of the time horizon, taking high values e.g. 335 dB for ε=2.5, N=500 (see Fig. 4.2) and e.g. 854 dB for ε=1 and N=200. For stable systems diagrams calculated for different N values converges with $N\to\infty$. In practise $N\geq100$ is sufficient for most systems, although smaller N corresponds to lower resolution in frequency domain. The shape of both 2D (Fig. 4.2) and 3D (Fig. 4.1) diagrams are similar, although the values are different, due to differences in the length of the time horizon, which results in differences in the magnitude diagram for unstable systems.

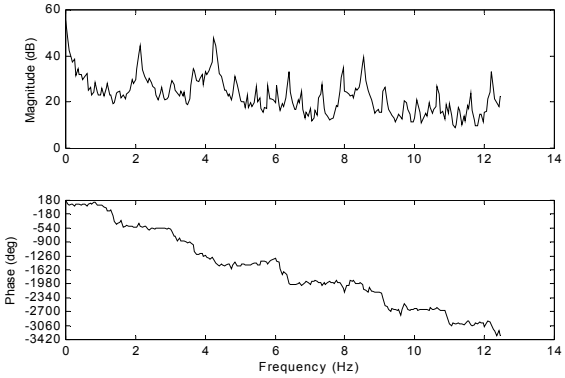

Fig. 4.3. Bode diagrams determined for discrete constant eigenvalues system (19-20) with parameters ε=2.93 and N=500.

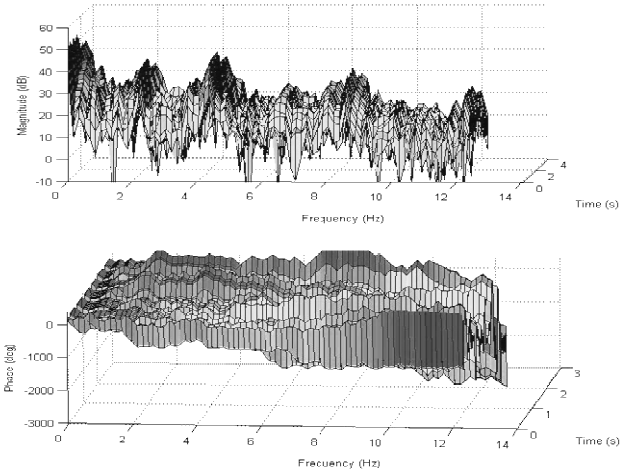

Fig. 4.4. 3D Bode diagrams determined for discrete constant eigenvalues system (19-20) with parameters ε=2.93 and N=150.

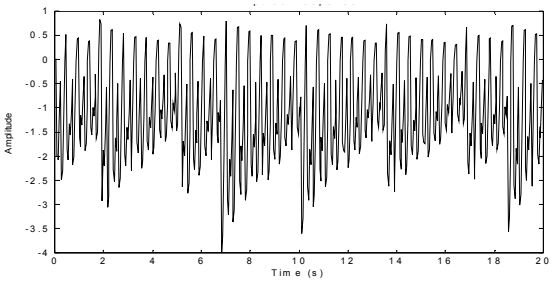

Fig. 4.5. Impulse response for system (19-20) with parameters ε=2.93, N=500, (open control loop).

For ε=2.93 the system is nearly at the boundary of stability. The amplification level on the Bode diagrams depicted in Fig. 4.3 is much more lower then for smaller ε e.g. ε=2.5. Furthermore the phase plot in Fig. 4.3 decrease in contrast to Fig. 4.2 where for unstable system, the phase increases.

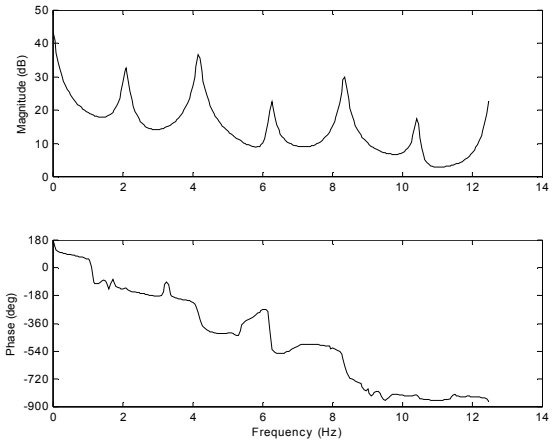

Fig. 4.6. Bode diagrams determined for system (19-20) with parameters ε=3 and N=500.

Moreover the surfaces depicted in Fig. 4.4 confirm the boundary character of the system, as they are discontinuous and the phase surfaces have no determinate direction for all time samples. Confirmation of stability/instability of the system in the time-domain may be impulse response plotted as in Fig. 4.5.

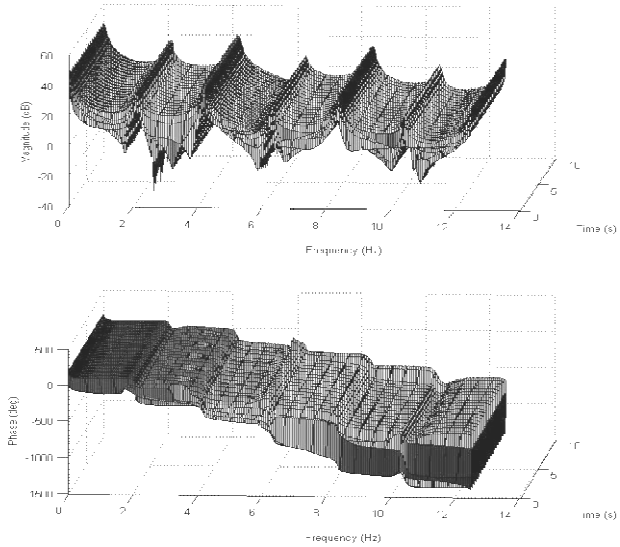

Fig. 4.7. 3D Bode diagrams determined for discrete constant eigenvalues system (19-20) with parameters ε=3 and N=150.

The next parameter value for which the system is analyzed is ε=3. Approximated Bode diagrams for such values are depicted in Fig. 4.6. The phase plot decreases, which is the first symptom of stability.

Similar observations can be done on 3D surfaces as depicted in Fig. 4.7. Here, the phase is again decreased and the magnitude is in the same range despite different values for N (500 and 150 steps, respectively).

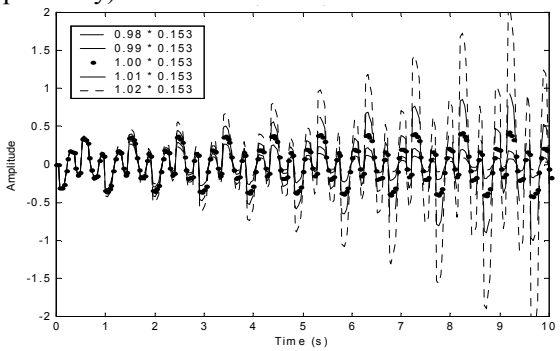

Fig. 4.8. Impulse responses for discrete constant eigenvalues system (19-20) with parameters ε=3, N=250, feedback loop and proportional controller k=0.1531 (-16.3dB).

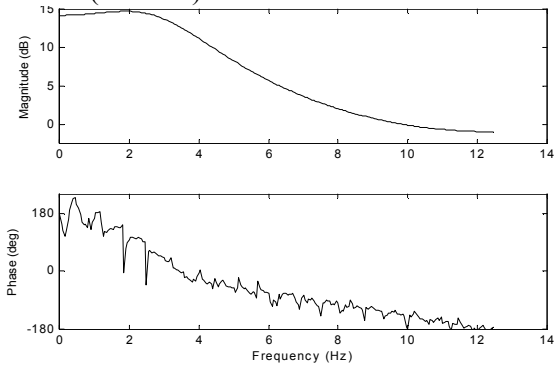

Fig. 4.9. Bode diagrams determined for discrete constant eigenvalues system (19-20) with parameters ε=20 and N=500.

The system without feedback is stable. Thus, it may be possible to find the lowest amplification of proportional controller for feedback control system that causes instability. Such amplification, found experimentally is equal to $k_{crit\_dB} = -16.3$ dB. The value is greater then corresponding amplification read out from Fig. 4.6 for the phase shift equal to 180 deg $-m_{dB} = -\left|G(f=0)\right| =$ -43 dB. Fig. 4.8 shows five impulse responses for a closed control loop system for amplification converted to linear scale k_{crit}=0.153 and similar gains to k_{crit} (differences are equal to $\pm 1\%$ and $\pm 2\%$ on a linear scale).

For ε=20 the system without feedback is also stable. Confirmation of this stability are Bode diagrams as depicted on Fig. 4.9, 4.10, 4.11.

Similar to previous examples one can find the critical gain for feedback control loop. Such amplification found experimentally is equal to $k_{crit\_dB} = -10.93$ dB. The value is greater than corresponding amplification read out from Fig. 4.9 $-m_{dB} = -\left|G(f=1.82)\right| =$ -14.7 dB for phase shifts equal to ± 180 deg. It should be noted that the difference is less than in the example with ε=3. A two-dimensional transfer function is depicted in Fig. 4.10, although it is much more difficult to estimate the critical gain using this plot.

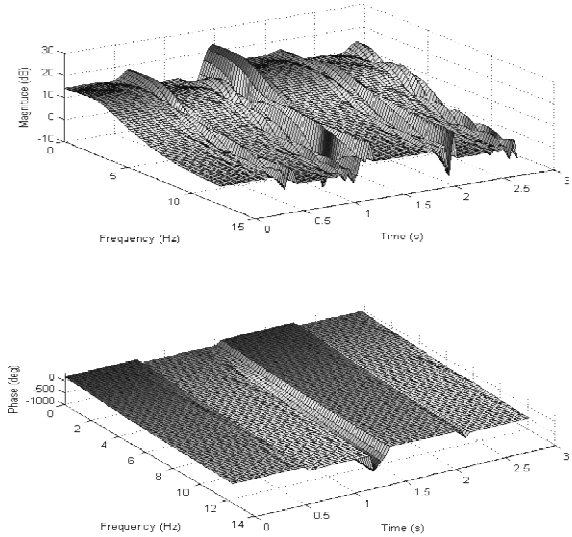

Fig. 4.10. 3D Bode diagrams determined for discrete constant eigenvalues system (19-20) with parameters ε=20 and N=150.

Fig. 4.11 gives information regarding linear time averaging of 2D-TF. The amplification level is quite different than that depicted on Figs. 4.9 and 4.10.

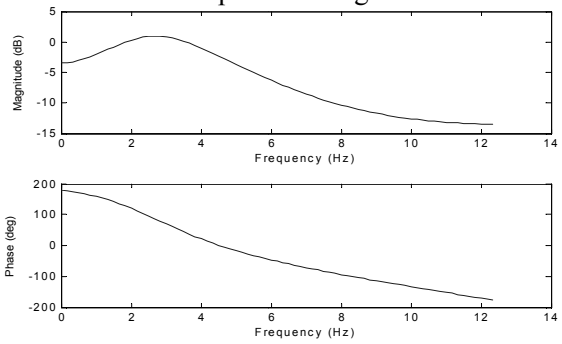

Fig. 4.11. Averaged 3D Bode diagrams complex on time domain for discrete constant eigenvalues system (19-20) with parameters ε=20, N=150.

Now we compare these diagrams with real amplification for sinusoidal input in following way. The input is sinusoidal with unitary amplitude and 5 different values of phase shift (0, 36, 72, 108, 144 deg). Magnification is calculated as output amplitude of respective input frequency, other components are omitted. Result of such comparison is depicted in Fig. 4.12. The thin dotted line shows real sin->sin magnifications, the thick continuous line is the averaged magnitude copied from Fig. 4.11. It can be seen that averaged Bode diagrams from Fig. 4.11 are a good approximation of selective amplification for the sinusoidal component. It has also been shown that from the stability analysis point of view the SVD-DFT

diagrams better approximate behaviour of LTV systems.

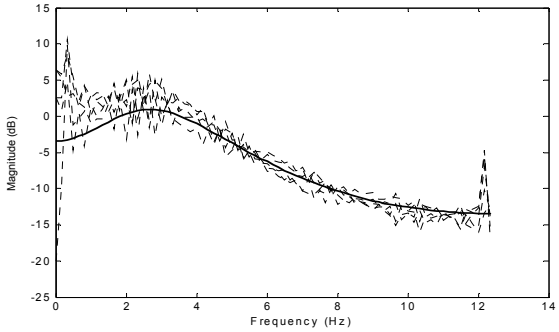

Fig. 4.12. Real magnifications of sinusoidal inputs for 5 different phase shifts for discrete constant eigenvalue system (19-20) with parameters ε=20, N=150.

Three impulse responses for closed control loop system (ε=20) are shown in Fig. 13. Amplification – 10.93 dB is converted to linear scale where k_{crit}=0.284 and gains are similar to k_{crit} (differences are equal to ±5% on a linear scale).

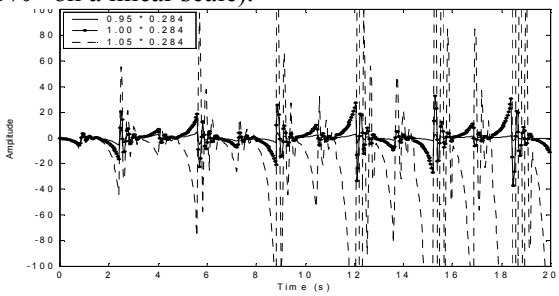

Fig. 4.13. Impulse responses for discrete constant eigenvalues system (19-20) with parameters ε=20, N=500, feedback loop and proportional controller (gain –10.93 dB).

5. CONCLUSION

Comparison of the three frequency domain methods for DT-LTV systems investigate and explore the most significant properties of each method as follows:

A. Using the 2-D transfer function one can explore the largest possible amount of information about the system. It can be read from any of the 3-D plot (figs. 4.1, 4.4, 4.7, 4.10) not only relation of magnitude and frequency, but also the period and the character of the system parameters variations. The main disadvantage of the method is the difficulty with analysing large amount of information, especially 3D plots, for which is also required higher computational power.

B. Analysed example shows that, modal parameters cannot be successfully applied for analysed system. Calculated parameters are constant and independent on the system properties controlled by parameter ε. Such results may be useful only for slow-varying systems, e.g. for large values of ε. Computed value of eigen-frequency may be in some sense representative only for the last case ε=20, where the corresponding maximum (f≈2.6 Hz) is also visible on Bode 2D diagrams fig. 4.9 and 3D surfaces fig. 4.10.

C. The method based on SVD-DFT is one-dimensional simplification of the LTV system. Creating and analysis of results on 2D plots is much more easier then on 3D surfaces. It is useful for simplified analysis of LTV systems. The stability results are more adequate for the SVD-DFT approximation however linear time-averaging of 2D transfer function (fig. 4.11) is closer to real sinusoidal magnification. Also it should be mentioned that the SVD-DFT method is in general only homogeneous because the computational algorithm (17-18) take advantage of power spectral density properties (13) and compute quadratic mean. On the other hand 2D-TF is linear (homogenous and additive) as well as ATF.

REFERENCES

[1] P. Gurfil (2003). Quantitative Lp Stability Analysis of a Class of Linear Time-Varying Feedback Systems. Int. J. Appl. Math. Comput. Sci., Vol. 13, No. 2, 179–184.

[2] S Songschon, W Richard (2003). Comparison of the stability boundary and the frequency response stability condition in learning and repetitive control, Int. J. Appl. Math. Comput. Sci., vol. 13, no. 2, 169–177

[3] Zadeh, L. A. (1950). Frequency analysis of variable networks. Proceedings of the Institute of Radio Engineers. 38, 291-299.

[4] P. Orłowski (2007). Frequency Domain Analysis of Uncertain Time-Varying Discrete-Time Systems. Circuits, Systems and Signal Processing.

[5] Liu, K. (1999). Extension of modal analysis to linear time-varying systems. Journal of Sound and Vibration 226, 149-167.

[6] Orlowski, P. (2004). Selected problems of frequency analysis for time-varying discrete-time systems using singular value decomposition and discrete Fourier transform. Journal of Sound and Vibration. Vol. 278, pp. 903-921.

[7] P. Orłowski (2007), An extension of Nyquist feedback stability for linear time-varying, discrete-time systems. Int. J. Factory Autom., Robotics and Soft Comp., Issue 2, pp. 51-56.

[8] P. Orłowski, An extension of Nyquist feedback stability for linear time-varying, discrete-time systems. *In book* Emerging Technologies, Robotics and Control Systems Vol. 1. International SAR, Palermo 2007, pp. 105-110.

[9] Matz G., Hlawatsch F. (1998) Time-frequency transfer function calculus of linear time-varying systems based on generalized underspread theory. J. Math. Physics, vol. 39, no. 8 pp.4041-4070.